JOURNAL OF VIROLOGY, Mar. 1992, p. 1602–1609
0022-538X/92/031602-08$02.00/0

Vol. 66, No. 3

Sequence and Structural Elements That Contribute to Efficient Encephalomyocarditis Virus RNA Translation

GREGORY M. DUKE,† MICHAEL A. HOFFMAN, AND ANN C. PALMENBERG*

Institute for Molecular Virology and Department of Veterinary Science, University of Wisconsin, Madison, Wisconsin 53706

Received 23 August 1991/Accepted 25 November 1991

The nucleotide sequence of the 5′ nontranslated region of encephalomyocarditis virus (EMCV-Rueckert) was determined, and a consensus RNA structural model for this sequence (850 bases) and three other poly(C)-containing cardioviruses (mengovirus, EMCV-B, and EMCV-D) was created through reiterative use of a minimum-free-energy folding algorithm. The RNA elements within this region which contribute to translation of EMCV proteins were mapped in cell-free reactions programmed with cDNA-derived RNA transcripts. The data provide evidence that stem-loop motifs I, J and K, formed by viral bases 451 to 785, are important components of cap-independent translation. In contrast to other reports, a minimal role for stem-loop H (bases 406 to 444) in translational activity is indicated. Small 5′ nontranslated region fragments (bases 667 to 797) containing the J and K motifs proved strong competitive inhibitors when added to cell-free reactions programmed with exogenous capped or uncapped mRNAs. The putative sequestering of required translational factors by this segment clearly contributes to translational activity, but also suggests a possible competitive mechanism for the down regulation of host protein synthesis during viral infection.

Unlike most eucaryotic mRNAs, the positive-strand genomes of picornaviruses are uncapped and have very long 5′ nontranslated regions (600 to 1,300 bases), which contain extensive secondary structure and multiple noninitiating AUG triplets (9, 36). These uncommon features, combined with the knowledge that poliovirus infection leads to inhibition of cap-dependent translation of normal cellular mRNAs, have long warranted suspicion about alternate translational mechanisms (9, 36). Our recent reports and those of others have indeed confirmed that 5′ non-translated regions (5′ NTRs) of poliovirus, encephalomyocarditis virus (EMCV) and foot-and-mouth disease virus promote cap-independent translation initiation, whereby ribosome binding occurs via internal entry onto the 5′ NTR without scanning from the 5′ terminus. Internal entry, relative to the 5′ terminus, has been clearly demonstrated with monocistronic and dicistronic cDNA-derived transcript RNAs (5, 10–12, 15, 16, 30), as well as with virion RNA (36). The binding site has been variously described as a ribosomal landing pad, translational enhancer, or internal ribosome entry site.

During poliovirus infection, cap-independent translation occurs in conjunction with viral 2A protease-induced degradation of cellular protein p220, a component of the eucaryotic initiation factor 4F (eIF-4F) cap-binding complex. The synergistic processes presumably promote viral translation while down regulating that of the host (18). Foot-and-mouth disease virus infection also induces degradation of p220, although a different viral protease (L rather than 2A) may be responsible (3). With EMCV, the translational shift from host to viral mRNA is likewise very proficient, but seems to result from a highly effective competition for cellular translational components rather than selective degradation of p220 (17, 21, 39).

The translational efficiency of EMCV RNA is especially apparent in cell-free extracts, in which 8 to 10 copies of viral polyprotein are typically obtained from each template (37). We have shown that the active nature of these templates is not unique to expression of viral coding sequences, but is a property that can be qualitatively transferred to nearly any eucaryotic cistron through ligation with viral fragments containing the internal ribosome entry site element (12, 27). The method has been widely used to obtain high-level protein expression in a variety of eucaryotic cells (5, 41). The transferred EMCV element usually includes bases 335 to 837 (translation begins at base 834) (5, 12), although deletion analyses with dicistronic chimeric mRNAs suggest that bases 403 to 811 may provide the core fragment for efficient translation (6, 14).

In this report, EMCV enhancer sequences are further defined through nested monocistronic RNA transcripts derived from cDNA clones and expressed in reticulocyte lysates. Linker insertion and deletion mapping show that translational functionality is achieved apparently through concerted contributions of several structures and sequences within the required region. Moreover, the potent inhibitory effects of one particular stem-loop element (the J-K domain, bases 680 to 785) on exogenously translating capped mRNAs suggest further biological involvement in putative host-protein shutoff mechanisms during natural viral infection.

MATERIALS AND METHODS

Sequence determination. EMCV Rueckert strain (EMCV-R) was passaged in HeLa cells, and vRNA was purified as described previously (33). Comprehensive sequence data for the 5′ noncoding region of EMCV-R were generated by three separate techniques: (i) primer extension dideoxynucleotide reactions with reverse transcriptase, using EMCV vRNA templates and 5′-labeled (^{32}P or ^{35}S) oligonucleotide primers; (ii) Maxam-Gilbert determinations of cDNAs synthesized from EMCV vRNA [poly(C) region]; and (iii) primer extension dideoxynucleotide reactions with Klenow polymerase, using EMCV cDNA-containing plas-

* Corresponding author.
† Present address: Department of Microbiology/Immunology, Stanford University, Stanford, CA 94305-5402.

mids as templates (20, 25, 38). All nucleotides were confirmed by multiple determinations.

A consensus RNA secondary structure for the 5′ noncoding regions of poly(C)-containing cardioviruses was created through reiterative use of the folding algorithm of Zuker and Stiegler (42), modified to accept large (e.g., >2,500 nucleotides) data fields. The minimum-free-energy structures for the 5′-most 2,500 nucleotides from EMCV-R, mengovirus-M (24), EMCV-D, and EMCV-B (1, 2), were calculated separately and then compared. The folding energies were those defined by Freier et al. (7) and averaged to about −1,180 kcal/mol (ca. −4,937 kJ/mol) for each sequence. Elements common to all determinations were retained, and intervening segments were refolded until a consensus structure maximizing total paired nucleotides in analogous configurations for all strains was achieved. The model was adjusted until the calculated minimum free energy did not differ by more than 5% from any of the optimum individual sequence solutions.

Construction of cDNA. Standard DNA cloning reactions (34) were used, and *Escherichia coli* JM101 was the bacterial host for propagation of recombinant DNA. The transcription vector Bluescribe M13+ was purchased from Stratagene. Plasmid pEA1, a subclone of pE13 (4), contained EMCV bases 335 to 4229 inserted between the *Eco*RI and *Bam*HI sites of Bluescribe M13+. This construction is very similar to plasmid pE5A1 (28), except for the choice of vector sequences. The pBalA1 plasmids (numbered 1 to 14) were derived from pEA1 and contained a nested series of sequential deletions (from progressive *Bal* 31 reactions) within the 5′ noncoding segments of the viral cDNA. Insertion mutations containing *Eco*RI restriction sites were made at naturally occurring *Mae*II restriction sites in the viral 5′ noncoding region of plasmid pEA1. The sequence at the insertion is ACGCGCGCGGAATTCGT (inserted sequences are underlined). Additional 4-base insertions were created by filling in *Avr*II and *Hin*dIII restriction sites within the viral 5′ noncoding region of pEA1 with Klenow fragment. An insertion-deletion plasmid was made by joining (with *Eco*RI linkers) sequences cleaved at *Kpn*I (base 701) and *Mae*II (base 776). The construction of all plasmids was confirmed by nucleotide sequencing.

Transcription of plasmid cDNA. Plasmid DNAs were linearized by digestion with *Bam*HI and used as templates in T7 polymerase runoff transcription reactions containing [α-^{32}P]CTP (13 mCi/mmol). Reactions were terminated by addition of EDTA (to 10 mM), and the samples were extracted with phenol-chloroform, precipitated with ethanol, and then resuspended in water. Reaction efficiency was monitored by scintillation counting after absorption of samples to Whatman DE81 filters. To determine the transcript size and purity, sample aliquots were denatured by incubation at 50°C for 1 h in the presence of 1 M deionized glyoxal and 10 mM Na_2HPO_4 (pH 6.5) and then loaded onto 1% agarose gels. After electrophoresis (1 V/cm for 11 h), dried gels were scanned for radioactivity with an Ambis radiation detector. The radioactivity in full-length transcript bands relative to that from the total sample was used to estimate the percentage of full-length RNA synthesized in the reaction.

In vitro protein synthesis. Cell-free translation reactions in reticulocyte extracts were performed as described previously (29). Typically, vRNA (1 to 3 μg) or transcript RNA (1 to 3 μg) was used to direct protein synthesis in reactions (15 to 30 μl) radiolabeled with [^{35}S]methionine (1 μCi/μl). After 60 to 90 min of incubation at 30°C, reactions were stopped by the addition of cycloheximide and pancreatic RNase (to 0.3 mg/ml each). Samples (3 μl) were analyzed by sodium dodecyl sulfate-polyacrylamide (Maizel) gel electrophoresis (SDS-PAGE) (26), and labeled proteins were visualized by autoradiography of the dried gel. Incorporation of [^{35}S]methionine into acid-insoluble products was performed as described previously (22).

```
   1  UUGAAAGCCGGGGGUGGGAGAUCCGGAUUGCCAGUCUGCUCGAUAUCGCAGGCUGGGUCC   60
  61  GUGACUACCCACUCCCCCUUUCAACGUGAAGGCUACGAUAGUGCCAGGGCGGGUACUGCC  120
 121  GUAAGUGCCACCCCAAAAUAACAACAGACCCCCCCCCCCCCCCCCCCCCCCCCCCCCCC  180
 181  CCCCCCCCCCCCCCCCCCCCCCCCCCCCCCCCCCCCCCCCCCCCCCCCCCCCCCCCCC  240
 241  CCCCCCCCCCCCCCCCCCCCCCUCUCCCUCCCCCCCCCCCUAACGUUACUGGCCGAAGCC  300
 301  GCUUGGAAUAAGGCCGGUGUGCGUUUGUCUAUAUGUUAUUUUCCACCAUAUUGCCGUCUU  360
 361  UUGGCAAUGUGAGGGCCCGGAAACCUGGCCCUGUCUUCUUGACGAGCAUUCCUAGGGGUC  420
 421  UUUCCCCUCUCGCCAAAGGAAUGCAAGGUCUGUUGAAUGUCGUGAAGGAAGCAGUUCCUC  480
 481  UGGAAGCUUCUUGAAGACAAACAACGUCUGUAGCGACCCUUUGCAGGCAGCGGAACCCCC  540
 541  CACCUGGCGACAGGUGCCUCUGCGGCCAAAAGCCACGUGUAUAAGAUACACCUGCAAAGG  600
 601  CGGCACAACCCCAGUGCCACGUUGUGAGUUGGAUAGUUGUGGAAAGAGUCAAAUGGCUCU  660
 661  CCUCAAGCGUAUUCAACAAGGGGCUGAAGGAUGCCCAGAAGGUACCCCAUUGUAUGGGAU  720
 721  CUGAUCUGGGGCCUCGGUGCACAUGCUUUACAUGUGUUUAGUCGAGGUUAAAAAACGUCU  780
 781  AGGCCCCCCGAACCACGGGGACGUGGUUUUCCUUUGAAAAACACGAUGAUAAUAUGGCCA  840
                                                    M  A  T
 841  CAACCAUGGAACAAGAGACUUGCGCGCACUCUCUCACUUUUGAGGAAUGCCCAAAAUGCU  900
        T  M  E  Q  E  T  C  A  H  S  L  T  F  E  E  C  P  K  C  S
 901  CUGCUCUACAAUACCGUAAUGGAUUUUACCUGCUAAAGUAUGAUGAAGAAUGGUACCCAG  960
        A  L  Q  Y  R  N  G  F  Y  L  L  K  Y  D  E  E  W  Y  P  E
 961  AGGAGUUAUUGACUGAUGGAGAGGAUGAUGUCUUUGAUCC 1000
        E  L  L  T  D  G  E  D  D  V  F  D
```

FIG. 1. Nucleotide sequence of the 5′-most 1,000 nucleotides of EMCV-R. The polyprotein reading frame begins at base 834, and the poly(C) tract contains 132 pyrimidines ($C_{115}UCUCCCUC_{10}$).

Nucleotide sequence accession number. The GenBank/EMBL accession number for this sequence (complete EMCV-R genome) is M81861.

RESULTS

Sequence and structure model for EMCV-R. The nucleotide sequence of the 5′-most 1,000 nucleotides of EMCV-R is presented in Fig. 1. The data correct minor discrepancies in the previous determination (23, 25) and complete the sequence for this strain. When poly(C) length differences are discounted, the 5′ NTR of EMCV-R shares 95.2% nucleotide identity with those of EMCV-B and EMCV-D (1, 2) and 92.7% identity with the same region from mengovirus-M (24).

A consensus RNA secondary structure for the 5′ ends of four cardiovirus RNAs, highlighting strain differences, is presented in Fig. 2. The model contains many elements similar to those suggested from partial sequence alignments (13, 31), but it also differs in three regards. First, these dominant patterns were derived from minimum-free-energy calculations which considered simultaneously all possible pairing options for large segments of the genome (the 5′-most 2,500 nucleotides). Second, the poly(C) tracts and their discontinuities were not excluded from consideration by the algorithm, but were allowed to (potentially) participate in base pairing, as long as these interactions could contribute to the lowest-energy solutions. Third, calculations from the final consensus model allowed a maximum deviation of only 5% from the optimum folding solution for each of the four participating (2,500-base) sequences. This model is consistent with most available data concerning enzyme-sensitive sites, exposed loops, etc., for related isolates of EMCV (6, 13, 31, 40).

The structure suggests a linear series of 5′ noncoding

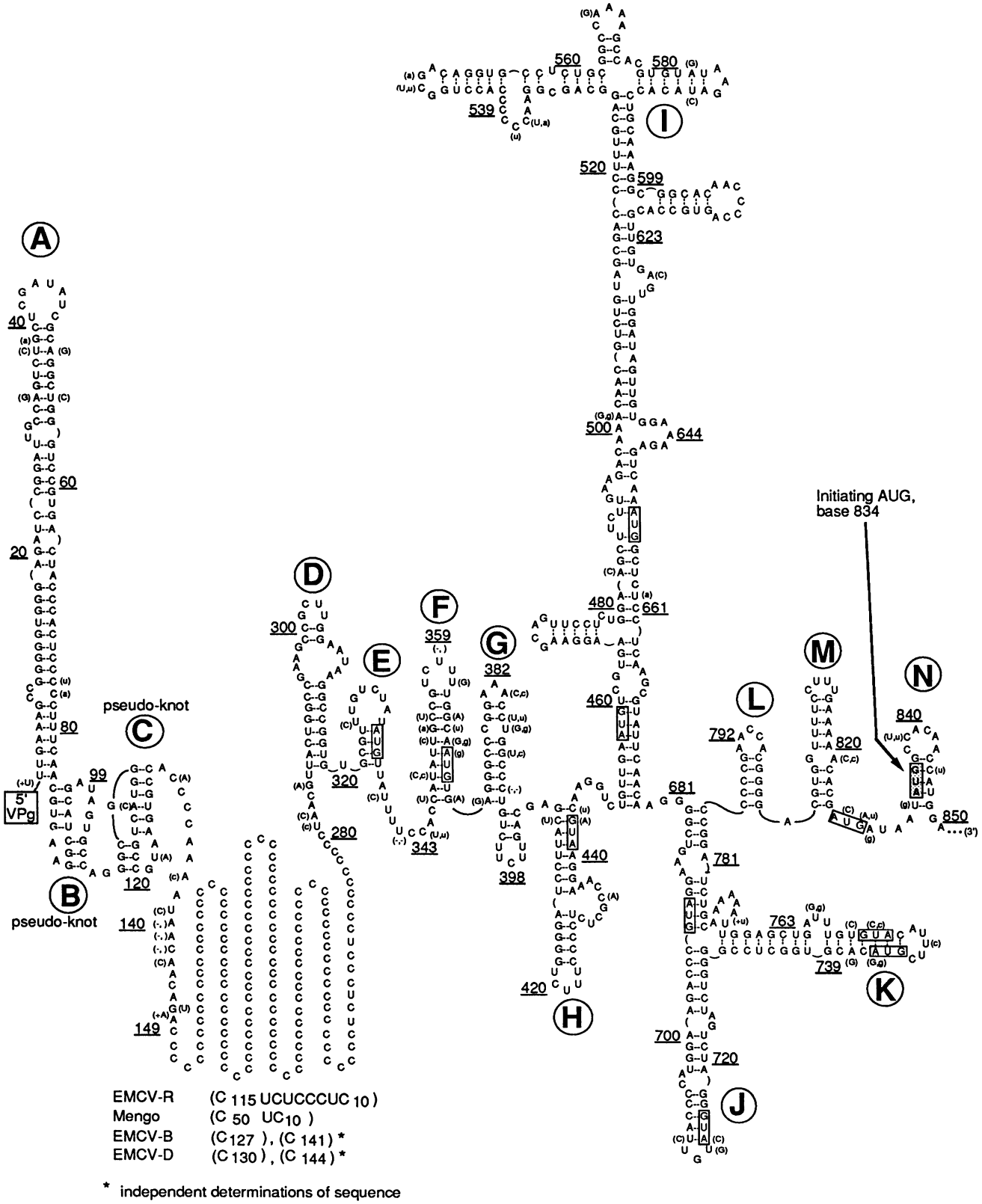

FIG. 2. Consensus secondary structure for 5′ NTRs of four related cardioviruses. The sequence shown is for EMCV-R. Changes in mengovirus and other EMCV strains (EMCV-B and EMCV-D) are given parenthetically as capital and lowercase letters, respectively. Stem-loop features are lettered consecutively, and AUG sequences (EMCV-R) are boxed.

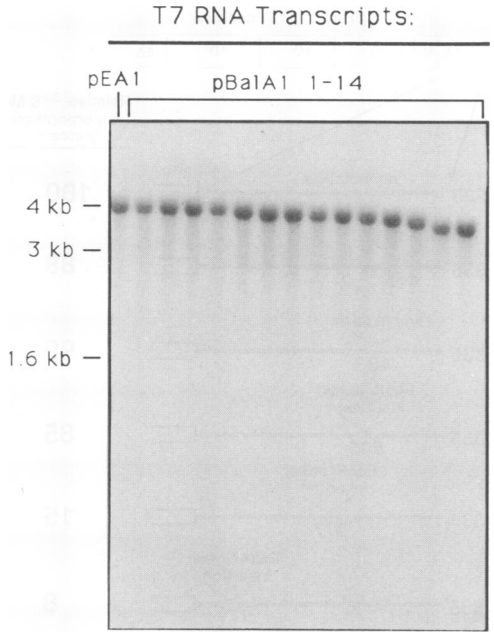

FIG. 3. RNA transcript integrity. T7 transcript samples from pBalA1-1 to pBalA1-14 were prepared, denatured, fractionated by electrophoresis, and detected as described in Materials and Methods.

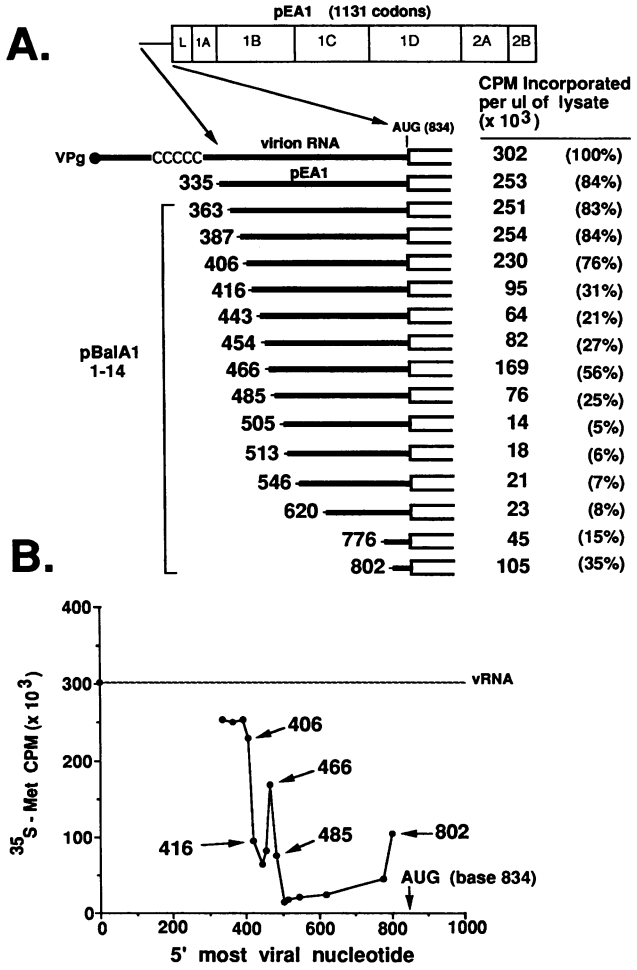

FIG. 4. 5′ deletion mutations. (A) EMCV virion RNA (1 μg) or T7 RNA transcripts (2.6 μg) as shown in Fig. 3 [pEA1 and pBalA1-1 to pBalA1-14] were used to program translation reactions (30 μl) in rabbit reticulocyte extracts containing [^{35}S]methionine (1 μCi/μl). After 90 min at 30°C, triplicate samples were removed (2 μl) and quantitated for trichloroacetic acid-insoluble radioactivity. Averaged results (standard deviation, <2%) are presented as counts per minute incorporated per microliter of lysate and also as percent incorporation relative to virion RNA. (B) Data from panel A displayed graphically.

stem-loop motifs (Fig. 2, letters A to N), within which at least 65% of the nucleotides [exclusive of the poly(C) tract] participate in base pairing. Surprisingly, the poly(C) region did not make a major contribution to the most favorable configuration of any sequence (5′-most 2,500 bases), even when allowed to pair with distant regions. The pseudoknot motifs in B and C differ from a published structure of this region (40), but this arrangement is energetically very favorable and has been independently suggested by algorithms sensitive to pseudoknot configurations (31a).

Among the considered viral strains, transitions (e.g., U→C or A→G) account for 60% of the sequence variation. More than two-thirds of these exchanges occur in stems and cause little (if any) perturbation of the common structure. The model has 10 examples of double substitutions within paired bases, although some of these compensating changes are separated by more than 40 to 50 nucleotides within the sequence (see stems A, F, H, I, and K). Transversions (e.g., U→A or G→C), insertions, and deletions are more common to the unpaired regions (77%) and are typically at the tops of stems or in bulge-loops between paired stems.

Translation of RNAs containing 5′ NTR mutations. To define important translational elements within the EMCV 5′ NTR, we constructed a series of cDNA plasmids containing progressive 5′→3′ deletions. The constructions, designated pBalA1-1 to pBalA1-14, each included coding sequences for the amino-terminal half of the polyprotein open reading frame (1,131 codons). RNA transcripts from these cDNAs were prepared in parallel and assayed by gel electrophoresis (Fig. 3) to ensure minimum variation in the amount of full-length material (ca. 70%). The transcripts were used to program reticulocyte lysate reactions, taking care that each sample received the same amount of RNA (2.6 μg), at a concentration (86 μg/ml) previously determined to give optimal, saturating protein synthesis.

The pEA1 transcripts which began at viral base 335 directed protein synthesis to about 84% of the level obtained with virion RNA. However, this is probably not a substantive difference in translational efficiency (6), since the truncated coding regions of the transcripts contain only half as many methionines (24 versus 51) as intact polyproteins. The pEA1 incorporation represents about three to five copies of protein product from each transcript template (pEA1), a significant activity considering the saturating concentrations of RNA, and provides the true baseline for comparison with other transcripts.

Engineered deletion of the next 52 viral bases (to base 387) gave transcript activities similar to those of pEA1 and confirmed previous observations that stem-loops A to G do not contribute significantly to EMCV translational functionality (12, 36). Further truncations, however, which impinged on structure H, showed significant decline in incorporation (Fig. 4B). Computer-generated structural models suggest that transcripts shortened within this region (i.e., beginning

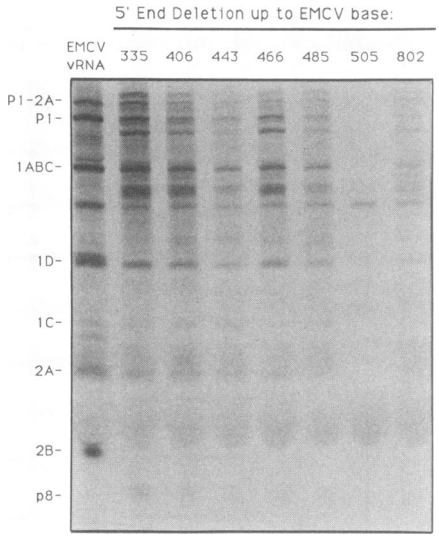

FIG. 5. Protein produced in cell extracts is viral. Samples from the translation extracts in Fig. 4 were processed with exogenous 3C protease and analyzed by SDS-PAGE and autoradiography.

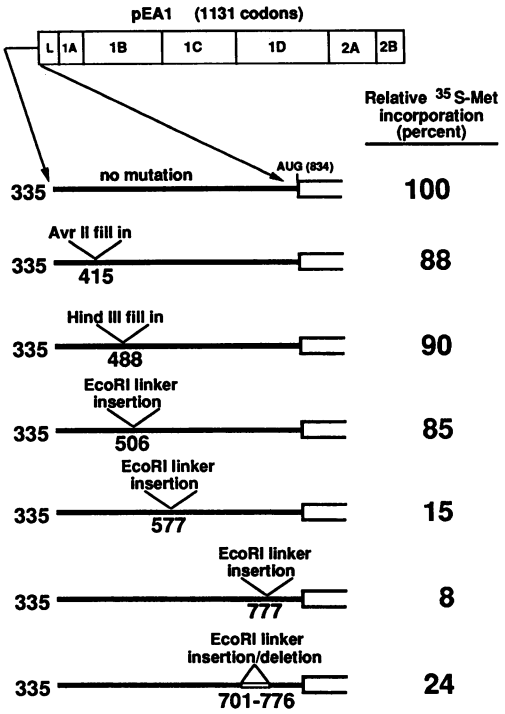

FIG. 6. Local insertion and deletion mutations. Mutations were created in pEA1 through restriction enzyme digest (*Avr*II at base 415; *Hin*dIII at base 488; *Mae*II at bases 506, 577, and 777; or *Kpn*I at base 701) followed by *Eco*RI linker insertion, filling in with Klenow polymerase, or sequential digestion (with *Kpn*I and *Mae*II) and *Eco*RI linker insertion. T7 RNA transcripts synthesized from these cDNAs (1.6 to 1.7 μg) were translated in reticulocyte lysates (15 μl) as in Fig. 4, and protein synthesis was quantitated by trichloroacetic acid-insoluble radioactivity. Presented values are relative to unmutated pEA1 transcript incorporation (ca. 250,000 cpm/μl), which was set at 100%.

with bases 406 to 450) may assume stable pairing configurations quite dissimilar to the consensus structure (not shown). The predicted alterations would disrupt stem-loop I as well as remaining H fragment, but it is also anticipated that slightly larger deletions (i.e., to bases 451 to 500) might restore most of the I configuration (see also reference 6). Indeed, complete removal of the H domain (to base 466) from the pBalA1-7 transcript partially reestablished translation in a reproducible manner. This level of incorporation was always lower (e.g., 56 versus 84%) than that achieved with pEA1, but clearly indicates that intact H sequences are not an absolute requirement for translational activity. Transcripts beginning with base 505, 513, 546, or 620 were poorly translated in the reactions, although very short transcripts with only 32 5′ NTR bases had somewhat better activity. These highly abbreviated RNAs (e.g., beginning with base 802) have been suggested to initiate synthesis in a 5′-end-dependent manner unrelated to internal ribosome entry site function (15).

The translation data presented in Fig. 4 were obtained with optimal concentrations of added template RNA. However, the differential levels of incorporation were clearly dependent on template sequence, not concentration, because similar results were also obtained under subsaturating RNA transcript conditions (e.g., 50 μg/ml), as long as compared samples contained similar molar equivalents of template (multiple determinations not shown).

To confirm that protein synthesis by the transcript series was uniformly initiating at the same AUG (base 834), we processed selected product samples with exogenous, unlabeled 3C protease and then analyzed them by SDS-PAGE (Fig. 5). Although the patterns varied in intensity according to incorporation, all lanes showed bands characteristic of L-P1-2AB* sequences and there was no clear evidence for significant levels of initiation at alternate AUG triplets. Even the shortest transcripts, which are missing major portions of the internal ribosome entry site, seemed to direct most residual synthesis towards the correct, in-frame AUG and hence reinforce findings that sequences and/or structures in the immediate vicinity of this codon probably play strong selective roles in synthesis initiation (15).

The deletion experiments placed the 5′ boundary for minimum translational activity within the lower regions of stem-loop I (roughly between bases 466 and 505). Local perturbations affecting this region were examined with engineered linker insertions or internal deletions (Fig. 6). Four-base insertions at position 415 (stem H) or 488 (lower stem of I) decreased translation of the downstream cistron by only 10 to 12%, consistent with the idea that an intact H element and the lower portion of stem-loop I are not required for translational functionality. Since deletions past base 485 gave virtually inactive templates (Fig. 4), it was surprising that insertions creating an extended bulge loop at base 506 were quite effective templates; this suggests that sizable alterations in the middle of stem I may also be tolerable, if stem integrity is generally maintained. In contrast, insertion at position 577, which disrupts the top of this stem (from bases 527 to 591), strongly decreased translational activity.

The J-K domain also contributes to efficient translational function. Deletions within this region (e.g., bases 701 to 776) or insertional augmentation near the A-rich bulge loop at base 777 significantly decreased protein synthesis (Fig. 6). The detrimental effects occurred without alteration of (predicted) base pairs within adjacent stems (H, I, L, M, etc.) and are consistent with data implicating this region as a required translational element and possible protein-binding site (35).

Translation competition assays. Cardiovirus RNAs have

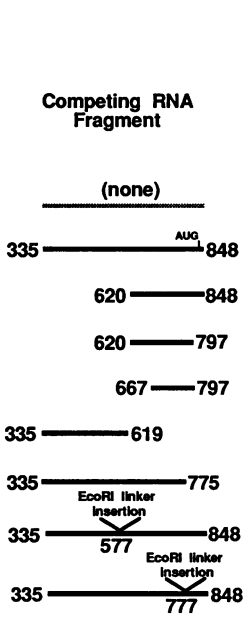

Competing RNA Fragment	Relative Incorporation (percent) of 35S-Met in Presence of Competing RNA: Template RNA FHV RNA (capped)	β-globin (capped)	pEA1 (EMCV)
(none)	100	100	100
335–848	36	12	42
620–848	37	13	42
620–797	65	34	48
667–797	nd	44	52
335–619	88	95	114
335–775	71	72	125
335–577 (EcoRI linker insertion)–848	13	<5	20
335–777 (EcoRI linker insertion)–848	68	62	105

FIG. 7. Translation competition assays. T7-derived RNA transcripts containing the indicated EMCV 5′ NTR sequences were added to reticulocyte reactions (15 μl) in a four- to sixfold molar excess (or a two- to threefold molar excess with β-globin reactions) over the template RNA. The template RNAs were: flock house virus (FHV) RNA (1.2 μg), cellular β-globin mRNA (0.8 μg), and pEA1 T7 transcripts (1.8 μg). Synthesized protein was quantitated by trichloroacetic acid-insoluble radioactivity after 60 min of incubation at 30°C. The results (average of duplicate samples) represent incorporation (percent) relative to samples with no added competitor RNA (typically, for FHV 300,000 cpm/μl = 100%, for β-globin 125,000 cpm/μl = 100%, and for pEA1 250,000 cpm/μl = 100%). The results are reproducible to a standard deviation of 10%. nd, not done.

been demonstrated to be efficient competitors of other eucaryotic mRNAs in cell-free synthesis reactions (32). Regions within the EMCV 5′ NTR that might sequester proteins were investigated in translation competition assays. RNA transcripts containing bases 335 to 848 or subfragments thereof were added to reticulocyte extracts containing translation-competent mRNAs from flock house virus, rabbit β-globin, or intact pEA1 (Fig. 7). Except for 14 bases, coding sequences were omitted from the tested fragments to reduce interference from synthesized viral protein and to focus the assays on initial translation events rather than elongation. Since the molar ratios of the competing segments were deliberately kept low (molar ratio of 2 to 6), depression of protein synthesis to 50% of the level achieved in the absence of fragment was indicative of strong competition.

The assays revealed that intact 5′ NTRs (bases 335 to 848) and all smaller segments containing bases 667 to 797 were reasonably effective competitors. The common sequence within these fragments centers on the J-K region. Computer predictions suggest that these stems are conserved in all inhibitory RNAs and make it likely that J-K-specific sequestering of required translational components (35) is responsible for this effect. Both capped (flock house virus and β-globin) and uncapped (pEA1) templates were sensitive to competition, although β-globin RNA was much less refractory than pEA1 and could typically be inhibited by lower molar ratios of fragment. With all templates, inhibition was less pronounced with the fragment from bases 335 to 775 or when the competitor included a 13-base insertion at base 777 (within J-K). The fragment from bases 335 to 619 had almost no inhibitory effect, which makes it unlikely that the observed results were a nonspecific consequence of added RNA. The relative inhibitory activity of the tested fragments was also evident at higher and lower molar excess of competitor RNAs (e.g., molar ratios of 1, 2.5, and 10) and confirm a dependence on sequence, rather than concentration (all data not shown).

DISCUSSION

Translation is initiated on picornavirus RNA by cap-independent, internal entry of ribosomes onto the 5′ NTR. Previous analyses of EMCV bases involved in efficient translation were carried out predominantly with dicistronic mRNAs (14). We have further defined the required RNA sequences by deletion and insertion analysis with monocistronic mRNAs. Although our results generally agree with those of Jang and Wimmer (14), they do call into question the role of stem-loop H. These authors suggested that integrity of H correlates with translational efficiency of the downstream cistron in dicistronic mRNAs and also with the ability of a 57-kDa cellular protein to bind to this specific structure. However, their tested deletions within this region were less comprehensive than our pEA1Bal series, and we have created at least one transcript in which this entire domain is cleanly removed (deletion to base 466) and yet the RNA still translates with reasonable efficiency (70% of that of pEA1).

We can only speculate about the reasons for these experimental discrepancies. However, it might be considered that monocistronic and dicistronic contexts could place entirely different constraints on the ability of the 5′ NTR to initiate translation. Indeed, Jang et al. showed previously (12) that some EMCV deletion mutants are more effective in monocistronic than dicistronic contexts. Moreover, it is possible that engineered constructions which only partially remove a local RNA motif have unanticipated configuration effects on adjacent structural elements. Thus, certain transcripts, either monocistronic or dicistronic, could potentially exhibit altered activities independent of the deleted sequences. Computer-aided RNA folding supports this idea and suggests that the deletions within stem-loop H (to positions 421 and 425) performed by Jang and Wimmer (14) might have disturbed the natural folding of adjacent stem I, in a manner analogous to our pEA1Bal constructions which begin at base 406, 416, or 443. Insertions specific to stem-loop H (linker insertion at base 415) or removal of H without disruption of I (deletion of base 466) allowed us to independently assess these motifs and to map the 5′-most required translational element to the lower regions of stem I rather than stem-loop H.

Our data are in agreement with those of Shih et al. (36), who found that cDNA fragments hybridizing to nucleotides 420 to 449 caused only a slight translational inhibition of EMCV vRNA, whereas cDNAs hybridizing between nucleotides 450 and 834 caused a high degree of inhibition. Correlative results were also obtained with the related foot-and-mouth disease virus, in which the RNA region controlling translation appears to maintain the same basic structural pattern as that of EMCV (31). The foot-and-mouth disease virus analog of EMCV stem H was mutated such that the 57-kDa protein bound very weakly, yet translation was decreased only 50% when compared with that of unmutated transcript RNA (16, 18a, 19). This lends support to our

conclusion that the integrity of stem H does not seem crucial for proper translational function.

We suggest instead that the J-K element and the ever-present stem-loop I play more critical roles in translation initiation. Independent of other 5′ NTR regions, the J-K sequences (bases 667 to 797) were remarkably active in competitive inhibition assays. It is notable that linker insertions in stems I and J-K (at bases 577 and 777, respectively) both destroyed translational activity but showed quite distinct effects when used as inhibitors in the competition assays. The insertion at base 577 (stem I) was an active competitor, whereas the insertion at base 777 (stem J-K) had lost inhibitory activity. The terminal loop of stem K (CUUUA, bases 746 to 750) was recently reported as an efficient binding site for eucaryotic initiation factor eIF-2/2B (35), a protein complex presumed to function in initiator AUG recognition (8). Consistent with our data, a strong competitive J-K sequence-dependent sequestering of these required translational elements may explain the overall efficiency of EMCV fragments at directing protein synthesis. Moreover, such interactions could provide a plausible mechanism by which EMCV vRNA may outcompete host mRNAs for ribosomes or initiation factors (eIF-2/2B?) and effect shutoff of cellular protein synthesis during infection. We are currently examining the role of purified eIF-2 and eIF-2B on translational activity and specifically on J-K-dependent inhibition of exogenous mRNA translation.

ACKNOWLEDGMENTS

We thank Ding Shih for critical reading of the manuscript and Cornelis Pleij for corroborative data concerning pseudoknot structures B and C.

This work was supported by Public Health Service grant AI-17331 from the NIH.

REFERENCES

1. **Bae, Y. S., H. M. Eun, and J. W. Yoon.** 1989. Molecular identification of a diabetogenic viral gene. Diabetes **38**:316–320.
2. **Cohen, S. H., R. K. Naviaux, K. M. V. Brink, and G. W. Jordan.** 1988. Comparison of the nucleotide sequences of diabetogenic and nondiabetogenic encephalomyocarditis virus. Virology **166**: 603–607.
3. **Devaney, M. A., V. N. Vakharia, R. E. Lloyd, E. Ehrenfeld, and M. J. Grubman.** 1988. Leader protein of foot-and-mouth disease virus is required for cleavage of the p220 component of the cap-binding protein complex. J. Virol. **62**:4407–4409.
4. **Duke, G. M., and A. C. Palmenberg.** 1989. Cloning and synthesis of infectious cardiovirus RNAs containing short, discrete poly(C) tracts. J. Virol. **63**:1822–1826.
5. **Elroy-Stein, O., T. R. Fuerst, and B. Moss.** 1989. Cap-independent translation of mRNA conferred by encephalomyocarditis virus 5′ sequence improves the performance of the vaccinia virus/bacteriophage T7 hybrid expression system. Proc. Natl. Acad. Sci. USA **86**:6126–6130.
6. **Evstafieva, A. G., T. Y. Ugarova, B. K. Chernov, and I. N. Shatsky.** 1991. A complex RNA sequence determines the internal initiation of encephalomyocarditis virus RNA translation. Nucleic Acids Res. **19**:665–671.
7. **Freier, S. M., R. Kierzek, J. A. Jaeger, N. Sugimoto, M. H. Caruthers, T. Neilson, and D. H. Turner.** 1986. Improved free-energy parameters for predictions of RNA duplex stability. Proc. Natl. Acad. Sci. USA **83**:9373–9377.
8. **Hershey, J. W. B., R. Duncan, and M. B. Mathews.** 1986. Introduction: mechanisms of translational control, p. 1–18. *In* M. B. Mathews (ed.), Translational control: current communications in molecular biology. Cold Spring Harbor Laboratory, Cold Spring Harbor, N.Y.
9. **Jackson, R. J.** 1986. A detailed kinetic analysis of the *in vitro* synthesis and processing of encephalomyocarditis virus products. Virology **149**:114–127.
10. **Jackson, R. J., M. T. Howell, and A. Kaminski.** 1990. The novel mechanism of initiation of picornavirus RNA translation. Trends Biochem. Sci. **15**:477–483.
11. **Jang, S. K., M. V. Davies, R. J. Kaufman, and E. Wimmer.** 1989. Initiation of protein synthesis by the internal entry of ribosomes into the 5′ nontranslated region of encephalomyocarditis virus RNA in vivo. J. Virol. **63**:1651–1660.
12. **Jang, S. K., H.-G. Krausslich, M. J. H. Nicklin, G. M. Duke, A. C. Palmenberg, and E. Wimmer.** 1988. A segment of the 5′ nontranslated region of encephalomyocarditis virus RNA directs internal entry of ribosomes during in vitro translation. J. Virol. **62**:2636–2643.
13. **Jang, S. K., T. Pestova, C. U. T. Hellen, G. W. Witherell, and E. Wimmer.** 1990. Cap-independent translation of picornaviral RNAs: structure and function of the internal ribosomal entry site. Enzyme **44**:292–309.
14. **Jang, S. K., and E. Wimmer.** 1990. Cap-independent translation of encephalomyocarditis virus RNA: structural elements of the internal ribosomal entry site and involvement of a cellular 57-kD RNA-binding protein. Genes Dev. **4**:1560–1572.
15. **Kaminski, A., M. T. Howell, and R. J. Jackson.** 1990. Initiation of encephalomyocarditis virus RNA translation: the authentic initiation site is not selected by a scanning mechanism. EMBO J. **9**:3753–3759.
16. **Kuhn, R., N. Luz, and E. Beck.** 1990. Functional analysis of the internal translation initiation site of foot-and-mouth disease virus. J. Virol. **64**:4625–4631.
17. **Lawrence, C., and R. E. Thach.** 1974. Encephalomyocarditis virus infection of mouse plasmacytoma cells. I. Inhibition of cellular protein synthesis. J. Virol. **14**:598–610.
18. **Lloyd, R. E., H. Toyoda, D. Etchison, E. Wimmer, and E. Ehrenfeld.** 1986. Cleavage of the cap binding protein complex polypeptide p220 is not effected by the second poliovirus protease 2A. Virology **150**:299–303.

18a. **Luz, N.** Personal communication.

19. **Luz, N., and E. Beck.** 1990. A cellular 57kDa protein binds to two regions of the internal translation initiation site of foot-and-mouth disease virus. FEBS Lett. **269**:311–314.
20. **Maxam, A. M., and W. Gilbert.** 1980. Sequencing end-labeled DNA with base-specific chemical cleavages. Methods Enzymol. **65**:499–560.
21. **Mosenkis, J., S. Daniels-McQueen, S. Janovec, R. Duncan, J. W. B. Hershey, J. A. Grifo, W. C. Merrick, and R. E. Thach.** 1985. Shutoff of host translation by encephalomyocarditis virus infection does not involve cleavage of the eucaryotic initiation factor 4F polypeptide that accompanies poliovirus infection. J. Virol. **54**:643–645.
22. **Palmenberg, A. C.** 1982. In vitro synthesis and assembly of picornaviral capsid intermediate structures. J. Virol. **44**:900–906.
23. **Palmenberg, A. C.** 1987. Comparative organization and genome structure in picornaviruses, p. 25–34. *In* M. A. Brinton, and R. R. Rueckert (ed.), Positive strand RNA viruses. Alan R. Liss, Inc., New York.
24. **Palmenberg, A. C., and G. M. Duke.** Unpublished data.
25. **Palmenberg, A. C., E. M. Kirby, M. R. Janda, N. L. Drake, G. M. Duke, K. F. Potratz, and M. S. Collett.** 1984. The nucleotide and deduced sequences of the encephalomyocarditis viral polyprotein coding region. Nucleic Acids Res. **12**:2969–2985.
26. **Palmenberg, A. C., M. A. Pallansch, and R. R. Rueckert.** 1979. Protease required for processing picornaviral coat protein resides in the viral replicase gene. J. Virol. **32**:770–778.
27. **Parks, G. D., G. M. Duke, and A. C. Palmenberg.** 1986. Encephalomyocarditis 3C protease: efficient cell-free expression from clones which link viral 5′ noncoding sequences to the P3 region. J. Virol. **60**:376–384.
28. **Parks, G. D., and A. C. Palmenberg.** 1987. Site-specific mutations at a picornavirus VP3/VP1 cleavage site disrupt in vitro processing and assembly of capsid precursors. J. Virol. **61**: 3680–3687.
29. **Pelham, H. R. B., and R. J. Jackson.** 1976. An efficient mRNA-

dependent translation system from reticulocyte lysates. Eur. J. Biochem. **67**:247–256.
30. **Pelletier, J., and N. Sonenberg.** 1988. Internal initiation of translation of eukaryotic mRNA by a sequence derived from poliovirus RNA. Nature (London) **334**:320–325.
31. **Pilipenko, E. V., V. M. Blinov, B. K. Chernov, T. M. Dmitrieva, and V. I. Agol.** 1989. Conservation of the secondary structure elements of the 5′-untranslated region of cardio- and aphthovirus RNAs. Nucleic Acids Res. **17**:5701–5711.
31a. **Pleij, C.** Personal communication.
32. **Rosen, H., G. Di Segni, and R. Kaempfer.** 1982. Translational control by messenger RNA competition for eukaryotic initiation factor 2. J. Biol. Chem. **257**:946–952.
33. **Rueckert, R. R., and M. A. Pallansch.** 1981. Preparation and characterization of encephalomyocarditis virus. Methods Enzymol. **78**:315–325.
34. **Sambrook, J., E. F. Fritsch, and T. Maniatis.** 1989. Molecular cloning: a laboratory manual, 2nd ed. Cold Spring Harbor Laboratory, Cold Spring Harbor, N.Y.
35. **Scheper, G. C., A. Thomas, and H. O. Voorma.** 1991. The 5′ untranslated region of encephalomyocarditis virus contains a sequence for very efficient binding of eukaryotic initiation factor eIF-2/2B. Biochim. Biophys. Acta **1089**:220–226.
36. **Shih, D. S., I.-W. Park, C. L. Evans, J. M. Jaynes, and A. C. Palmenberg.** 1987. Effects of cDNA hybridization on translation of encephalomyocarditis virus RNA. J. Virol. **61**:2033–2037.
37. **Shih, D. S., C. T. Shih, D. Zimmern, R. R. Rueckert, and P. Kaesberg.** 1979. Translation of encephalomyocarditis virus RNA in reticulocyte lysates: kinetic analysis of the formation of virion proteins and a protein required for processing. J. Virol. **30**:472–480.
38. **Smith, A. J. H.** 1980. DNA sequence analysis by primed synthesis. Methods Enzymol. **65**:560–580.
39. **Svitkin, Y. V., V. A. Ginevskaya, T. Y. Ugarova, and V. I. Agol.** 1978. A cell-free model of the encephalomyocarditis virus-induced inhibition of host cell protein synthesis. Virology **87**: 199–233.
40. **Vartapetian, A. B., A. S. Mankin, E. V. Shripkin, K. M. Chumakov, V. D. Smirnov, and A. A. Bogdanov.** 1983. The primary and secondary structure of the 5′ end region of encephalomyocarditis virus RNA. A novel approach to sequencing long RNA molecules. Gene **26**:189–195.
41. **Zhou, Y., T. J. Giordano, R. K. Durbin, and W. T. McAllister.** 1990. Synthesis of functional mRNA in mammalian cells by bacteriophage T3 RNA polymerase. Mol. Cell. Biol. **10**:4529–4537.
42. **Zuker, M., and P. Stiegler.** 1981. Optimal computer folding of large RNA sequences using thermodynamics and auxiliary information. Nucleic Acids Res. **9**:133–148.